

論文内容の要旨

論文題目 Structural and photoelectrochemical behavior of
self-assembled Ag/Co nanostructures
embedded in TiO₂ thin films

(TiO₂ 薄膜中の自己組織化 Ag/Co ナノ構造の構造及び光
電気化学特性)

氏名 渡部 愛理

Introduction

Nanocomposite materials composed of metal nanoparticles and a dielectric matrix have attracted significant attention from both fundamental and application aspects because of their unique optical, electronic, catalytic, and magnetic properties^[1]. Especially Ag nanostructures exhibit large optical electric-field enhancement in the visible wavelength region due to small imaginary part of its dielectric constant^{[2], [3]}. For example, Tian *et al.*^[4] reported that Ag nanostructures catalytically loaded on the nanoporous TiO₂ films showed four times higher conversion efficiency than TiO₂ films with Au nanoparticles. However Ag in plasmonic devices generally has a serious problem that the Ag nanoparticles easily and quickly sulfidate and oxidate in air. Recently, Ikemiya *et al.*^[5] reported that nanomatch-like Ag-Co hybrid nanostructures, consisting of Ag nanorods and Co nanoparticles, can be embedded in anatase TiO₂ matrix by PLD. The absorption spectrum of the Ag-Co-TiO₂ nanocomposite film exhibited a localized surface plasmon resonance (LSPR) peak at ~450 nm in wavelength^[5]. It is noteworthy that the Ag nanostructure embedded in TiO₂ matrix is stable in the ambient air for several months. The Ag-Co-TiO₂ nanocomposite film has potential applications in plasmonic devices such as biosensors and photovoltaic cells. The device performance is, in general, sensitive to the shape, size, and distribution of metal nanostructures. Thus, it is important to control the size and density of Ag-Co hybrid nanostructures during film growth. In this study, I first investigated the structural variation of Ag-Co nanostructures with substrate temperature (T_s) during deposition and the Ag amount in Ag-Co-TiO₂ nanocomposite films. Next I conducted photocurrent measurements of the Ag-Co-TiO₂ nanocomposite film, in order to demonstrate the potential of the nanocomposite film as an electrode in plasmonic photo-electrochemical cells.

Experimental section

I. Structural variation of Ag-Co nanostructures

Nanocomposite films of $\text{Ag}_x\text{Co}_5(\text{TiO}_2)_{95}$ ($x = 20, 40, 60,$ and 80) were fabricated on LaSrAlO_4 (LSAO) (001) substrates by PLD, where x is the nominal composition. A KrF excimer laser operating at 2 Hz and with energy 18 mJ/pulse was used for ablation. Sintered pellets of pure TiO_2 and $\text{Ag}_x\text{Co}_5(\text{TiO}_2)_{95}$ (molar ratio of $\text{Ag}:\text{Co}:\text{TiO}_2 = x:5:95$) were used as PLD targets for fabricating TiO_2 seed layers and $\text{Ag}_x\text{Co}_5(\text{TiO}_2)_{95}$ films, respectively. A pure anatase TiO_2 seed layer was first deposited on the LSAO substrate at $650\text{ }^\circ\text{C}$ under an oxygen pressure (P_{O_2}) of 5×10^{-3} Torr. Subsequently, a $\text{Ag}_x\text{Co}_5(\text{TiO}_2)_{95}$ thin film was deposited on the seed layers at $T_s = 250\text{--}350\text{ }^\circ\text{C}$ and $P_{\text{O}_2} = 1 \times 10^{-6}$ Torr. The crystal structures of the films were determined using X-ray diffraction (XRD) (Bruker, AXS with GADDS). Their absorption spectra were measured using an ultraviolet-visible spectrometer. Size and distribution of the Ag-Co nanostructures were characterized using scanning transmission electron microscopy (STEM) combined with energy-dispersive X-ray imaging (EDX).

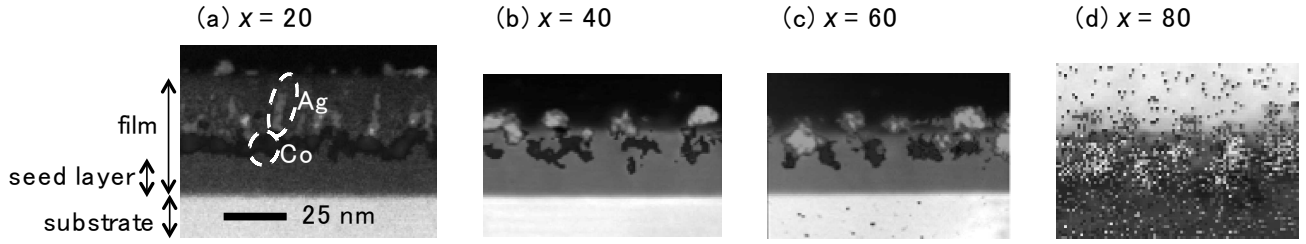
II. Photoelectric conversion using the characteristic nanomatch-like Ag-Co structures

I fabricated Ag-Co-TiO₂ nanocomposite films on Nb doped SrTiO₃ (Nb:STO) (100) conducting substrate in order to evaluate the photoelectric conversion efficiency. The aforementioned laser parameters were used. Sintered pellets of $\text{Ti}_{0.97}\text{Nb}_{0.03}\text{O}_2$ (Nb:TiO₂) and $\text{Ag}_{20}\text{Co}_5(\text{TiO}_2)_{95}$ were used as PLD targets for seed layers and Ag-Co-TiO₂ nanocomposite film, respectively. The Nb:TiO₂ seed layer and then a Ag-Co-TiO₂ nanocomposite film were deposited at $T_s = 650\text{ }^\circ\text{C}$ and $P_{\text{O}_2} = 1 \times 10^{-5}$ Torr, at $T_s = 300\text{ }^\circ\text{C}$ and $P_{\text{O}_2} = 1 \times 10^{-6}$ Torr, respectively. The composition of the Ag-Co-TiO₂ nanocomposite film was evaluated to by inductively coupled plasma-mass spectrometry (ICP-MS). Nanostructures of the films were investigated by STEM-EDX. Extinction spectrum measurements were performed using a microscopic absorption spectroscopic measurement system. Photoelectrochemical measurements were performed using a three-electrode electrochemical measurement system. The Ag-Co-TiO₂ film, a platinum wire and a saturated calomel electrode (SCE) were used as working, counter and reference electrodes, respectively^[6]. As an electrolyte solution, Ar saturated 0.1 M KClO₄ aqueous solution was used. A bandpass filter or a cut filter was used to select irradiation wavelength from a light source (Xenon lamp).

Results and discussions

I. Structural variation of Ag-Co nanostructures

The θ - 2θ XRD patterns of the $\text{Ag}_x\text{Co}_5(\text{TiO}_2)_{95}$ ($x = 20, 40, 60,$ and 80) thin films grown at $T_s = 300\text{ }^\circ\text{C}$ clearly show diffraction peaks at $2\theta = 38^\circ$, corresponding to the 004 plane of anatase. In addition, the 004 diffraction peak appeared as a spot in the 2θ - χ image measured by a two-dimensional detector, proving that anatase single-crystal phase was grown in all the films. No secondary phases such as Co and Ag were detected. Figures 1 (a)–(d) show cross-sectional STEM-EDX images of the films with various Ag content x grown at $300\text{ }^\circ\text{C}$. The film with $x = 20$ demonstrates the characteristic nanomatch-like structures composed of a Ag rod on Co sphere, as reported previously^[5]. The Ag-Co hybrid nanostructures were completely embedded in the TiO_2 matrix. In contrast, in the films with $x \geq 40$, the nanostructures changed their shape from rod-like to spherical. As x increases from 40 to 60, the size of the Ag nanoparticles increased. Furthermore, the Ag nanoparticles in the films with $x = 40$ and 60 were located near the film surface and partially embedded in the TiO_2 matrix, while the Co particles were likely to reside beneath the Ag particles. In the films with $x =$



Figures 1. (a)-(d): Cross-sectional STEM-EDX mapping images of $\text{Ag}_x\text{Co}_5(\text{TiO}_2)_{95}$ films grown at 300°C . Ag content, x , is (a) 20, (b) 40, (c) 60, and (d) 80. Distribution of Ag and Co inside the sample are depicted as white and black, respectively overlapped on highangle annular dark-field image ((a)-(c)) or bright-field image (d). Arrows beside the images are the guides show the areas of the film and the substrate, respectively.

80, the Ag nanoparticles became much larger; some of these particles were totally embedded while others were partially embedded in the TiO_2 matrix. In addition, Ag was spread over the entire TiO_2 film.

From these observations, it is clear that the nanomatch-like structures evolved only in a narrow x range of approximately 20. The cross-sectional STEM-EDX images of the $x = 20$ films grown at different T_s were obtained (data not shown). The film grown at $T_s = 250^\circ\text{C}$ exhibited similar nanomatch-like structures as those obtained at $T_s = 300^\circ\text{C}$. However, in the film fabricated at 350°C , no hybrid structure was observed. Irregular spherical shape Ag particles were distributed near the film surface. Therefore, it is concluded that the nanomatch-like structures are formed in the narrow temperature range $250\text{-}300^\circ\text{C}$.

Figure 2 shows the absorbance spectra of the $\text{Ag}_x\text{Co}_5(\text{TiO}_2)_{95}$ films with different Ag content grown at 300°C . A large absorption below 390 nm corresponds to the interband transition across the band-gap of TiO_2 . Broad LSPR peaks were observed in the visible wavelength region ($400\text{-}800\text{ nm}$). As x was increased, the peak intensity was enhanced, reflecting the increase in Ag density. Moreover the position of the LSPR peak systematically shifted to longer wavelengths. The red-shift of the peak is attributed to the increase in the Ag particle size.

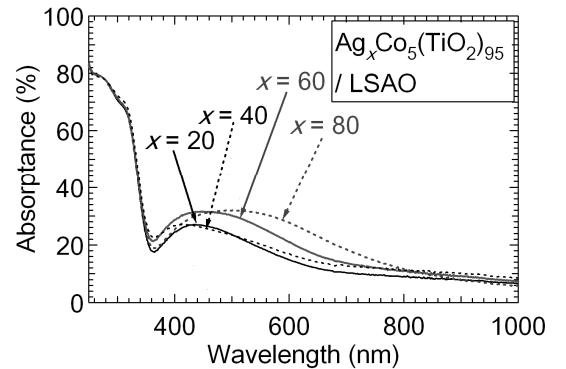


Figure 2. Absorbance spectra of the $\text{Ag}_x\text{Co}_5(\text{TiO}_2)_{95}$ films.

II. Photoelectric conversion using the characteristic nanomatch-like Ag-Co structures

The cross-sectional TEM-EDX image of the Ag-Co- TiO_2 films fabricated on the Nb: TiO_2 seed layer revealed that nanomatch-like structures were successfully obtained even on the conductive substrate Nb:STO.

According to the extinction spectrum of the film, a broad LSPR band of Ag nanostructures is seen around $400\text{-}600\text{ nm}$. The peak is broad because the lateral positions of silver nanorods are random. Although most of Co is segregated between Ag nanorods and substrate to form Co nanoparticles, Co nanoclusters of several nm scale also reside near the film surface, which prevent Ag

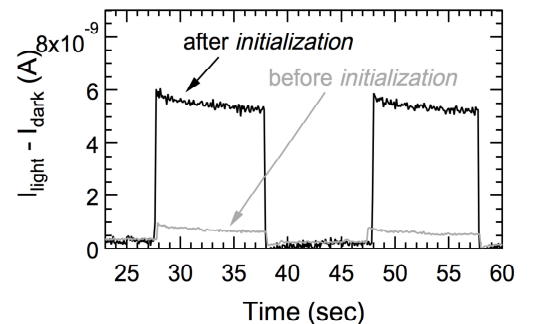


Figure 3. I - t curve of Ag-Co- TiO_2 film, before and after initialization.

nanorods from direct exposed to the air. Current was monitored, applying the 0.1 V versus saturated calomel electrode (SCE) with the 450 nm light on and off. The current of the Ag/Co nanocomposite film was not enhanced at all, compared with that of pure titania film without nanostructures. This is because the silver nanostructures are completely protected by the titania matrix and the surface cobalt nanoclusters on the top of silver nanorods. The Ag nanostructures need to be in contact with an electrolyte solution when the nanocomposite film is used for photoelectric conversion. I tried to remove the Co nanoclusters on the film surface by selective electrochemical oxidation of Co by charging 0.3 V vs. SCE for 100 s under dark condition. Hereafter I call this ‘unseal’ process Ag as initialization. Voltammograms (data not shown) were measured after the *initialization*, with and without irradiation of visible light ($420 < \lambda \leq 1300$ nm). Figure 3 shows that the *I-t* curve before *initialization* was almost same as that of pure TiO₂ film without Ag nanorods. Meanwhile, the photocurrent after *initialization* was enhanced by seven times. This proves that the Ag nanorods originally ‘sealed’ in TiO₂ matrix by surface Co clusters was successfully ‘unsealed’ by the *initialization* process. In order to investigate the photoelectric conversion properties, the incident photon-to-photocurrent efficiency (IPCE) of the film was obtained (Figure 4). Both spectra show similar behavior, i.e., increase of extinction/IPCE with decreasing wavelength below 600 nm. This strongly suggests that the photocurrent was enhanced by the effect of plasmon resonance. Accompanied with the observation of photocurrent, photooxidized Ag dissolved into water as a form of Ag⁺ ion.

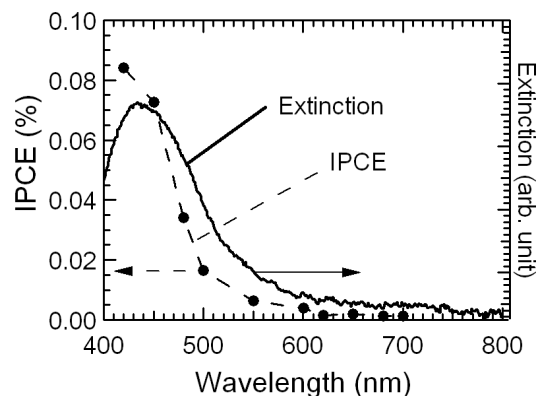


Figure 4. IPCE action spectrum and extinction spectrum of the Ag-Co-TiO₂ nano composite film.

Conclusions

I investigated the structural variation of Ag-Co nanostructures in Ag_xCo₅(TiO₂)₉₅ nanocomposite films with varying pulsed laser deposition conditions. Ag-Co nanomatch-like structures appeared only at a specific condition, and changed from rod-like to spherical with increasing *x*. A broad Ag LSPR peak systematically shifted to longer wavelengths with increasing *x*. In addition, I proposed the nanocomposite film with Ag-Co nanomatch-like structures embedded in TiO₂ matrix as a promising electrode material: this new structure does not merely protect Ag structure, but fresh Ag can be obtained when needed. I indeed made the Ag nanostructures contact with the supporting electrolyte, and subsequently observed photocurrent enhanced by plasmonic resonance of Ag nanorods. This Ag-Co-TiO₂ nanocomposite film would be useful in not only photoelectric conversion but also plasmonic sensor or catalysis, in which fresh Ag nanostructure is needed.

References

- [1] S. Komameni, *J. Mater. Chem.* **1992**, *12*, 1219,
- [2] U. Kreibig and M. Vollmer, *Optical Properties of Metal Clusters*, Springer-Verlag, **1995**,
- [3] K. L. Kelly, E. Coronado, L. L. Zhao, G. C. Schatz, *J. Phys. Chem. B.* **2003**, *107*, 668.,
- [4] Y. Tian, T. Tatsuma, *Chem. Commun.* **2004**, *16*, 1810.,
- [5] K. Ikemiya, K. Konishi, E. Fujii, T. Kogure, M. Kuwata-Gonokami, T. Hasegawa, **2013**, arXiv: 1309.6171 [cond-mat.mtrl-sci].
- [6] Y. Nishijima, K. Ueno, Y. Yokota, K. Murakoshi, H. Misawa, *J. Phys. Chem. Lett.* **2010**, *1*, 2031.,